REMOVAL OF RESIDUAL CHIRP IN COMPRESSED BEAMS USING A PASSIVE WAKEFIELD TECHNIQUE

M. Harrison*, G. Andonian, T. Campese, A. Murokh, F. H. O'Shea, M. Ruelas,
RadiaBeam Technologies, Santa Monica, CA 90404, USA
P. Frigola, RadiaBeam Systems, Santa Monica, CA 90404, USA
M. Fedurin, Brookhaven National Laboratory, NY 11961, USA

Abstract

The removal of residual chirp in XFELs is of paramount importance for efficient lasing. Although current S-band XFELs remove the unwanted residual chirp using off-crest acceleration after the final bunch compressor, this technique is not possible for XFELs with soft X-ray lines as there are no further accelerating structures. The off-crest dechirping technique is also expensive for future superconducting XFELs. In response, RadiaBeam Systems presents its work, building upon the theoretical work of Bane and Stupakov [1], in RF-free residual chirp mitigation using only passive techniques. Beam-induced longitudinal wakefields are produced with opposing corrugated plates which allow for an entirely RF-free chirp removal. Theory, engineering, and experimental results are presented.

INTRODUCTION

Beam dechirping is crucial for current and future XFELs. Accelerating and compressing sections of beamlines leave beam bunches with a residual chirp that must be removed for lasing. In the SLAC LCLS, dechirping requires hundreds of meters of off-crest accelerating structures. This is costly both in terms of accelerating cavity efficiency and beamline space [2].

RadiaBeam Systems has designed and manufactured a compact, low-cost corrugated plate system with an adjustable gap for tunable beam dechirping. Its dechirping characteristics were measured at the Brookhaven National Laboratory (BNL) Accelerator Test Facility (ATF).

THEORY

The driving theory for designing the passive dechirper system has been presented in papers by Bane, Stupakov, and Emma [2] [3]. The longitudinal wakefield generated by a single electron passing between the corrugated plates is given by

$$w(z) = \left(\frac{\pi^2}{16}\right)\frac{Z_0 c}{\pi a^2} H(z) cos\left(\frac{2\pi z}{\lambda}\right), \qquad (1)$$

where $Z_0 = \sqrt{\mu_0/\epsilon_0}$ is the impedance of free space, $H(z)$ is the unit step function, c is the speed of light, z is the coordinate along the beam path, and λ is the wavelength of the dominant mode of the wakefield given by

$$\lambda = 2\pi\sqrt{\frac{a\delta g}{2p}}. \qquad (2)$$

The remaining variables describe the dimensions of the corrugated plates. a is the distance of the plates from the beamline (half the plate separation); δ is the depth of the corrugations; g is the gap between corrugations; p is the period of the corrugations. These dimensions are listed in Table 1 and pictured in Figure 2. For compliance with the derivation assumptions, $p, d \ll a$ and $\delta \gtrsim p$ [2]. The transverse dimension of the plates is taken to be infinite.

The $\pi^2/16$ factor comes from the differing geometry between parallel plates and the circular pipe that was used in Stupakov and Bane's original derivation [4]. The wakefield produced by the bunch is found by convolving the single particle wakefield (Equation 1) with the longitudinal beam bunch charge density profile. For rectangular longitudinal profiles, the wakefield is linear in the region of the beam bunch as shown in Figure 1. For plates that satisfy the constraints above, the dechirping strength, h, is given by the slope of the linear region and can be calculated by

$$h = \left(\frac{\pi^2}{16}\right)\frac{Z_0 c Q L}{\pi a^2 l}, \qquad (3)$$

where Q is the bunch charge, L is the length of the dechirper, and l is the bunch length.

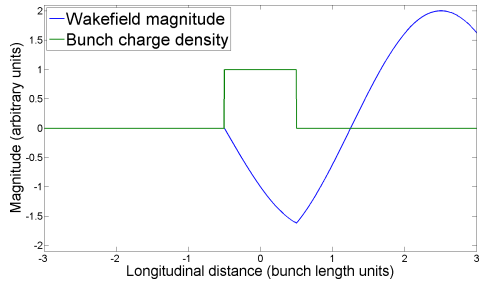

Figure 1: Bunch current profile and generated longitudinal wakefield.

CORRUGATED PLATE DIMENSIONS AND MANUFACTURE

The dimensions of the corrugated plates used in this experiment are listed in Table 1. The plates were fabricated

* harrison@radiabeam.com

ISBN 978-3-95450-138-0

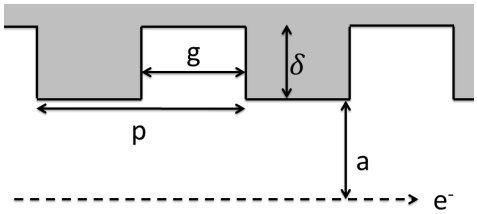

Figure 2: Diagram of corrugated plates.

Table 1: Corrugated Plate Dimensions

Dechirper dimensions			
Length	L	181	mm
Width		38.1	mm
Period	p	1.15	mm
Depth	δ	1.15	mm
Gap	g	0.77	mm
Plate separation	a	1–30	mm
Material		Aluminum	

from aluminum for its light weight and ease of machining. Note that the conductivity of the plates does not affect the function of the dechirper as long as the fundamental mode of the wakefield is dominant [5].

The plates were actuated by stepper motor-driven linear motion feedthroughs–one at each end of each plate. This allows for control of the plates' vertical position, separation, longitudinal angle, and alignment with the beam. Figure 3 shows the corrugated plates and the attachments to the linear actuators above. Figure 4 shows a close-up of the plates after alignment.

PROCEDURE

The plates were installed in a box chamber on Beamline 2 at the BNL ATF and were aligned to the beam using an alignment laser. The beam parameters for the experiment are given in Table 2.

The measured dechirping strength (h in Equation 3) of a configuration is defined as the change in energy spread divided by the bunch length. A beam with a known bunch length and energy spread was passed between the plates. As the plate separation was varied, the change in energy spread was measured by a downstream energy spectrometer. Photographs of the plates (e.g., Figure 4) taken with a calibrated camera are used to measure the separation.

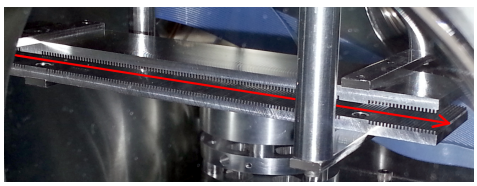

Figure 3: Full view of dechirper as installed. The red arrow indicates the electron beam path.

Table 2: BNL ATF Beam Properties

BNL ATF beam parameters			
Beam energy	E	57.6	MeV
Bunch charge	Q	340	pC
Initial chirp		400	keV/mm
Transverse beam size		100	microns
Pulse length (full width)	l	3.4	psec
Longitudinal profile		Rectangular	

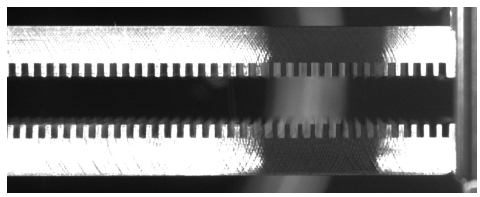

Figure 4: Side view of corrugated plates. Beam travels left to right. Note the corrugations are longitudinally misaligned by about a quarter of a period.

Bunch charge is measured by a downstream Faraday cup.

In a second round of measurements, the bunch charge was scanned at a fixed plate separation of 3.90 mm.

RESULTS

A selection of energy spectrum measurements at various plate separations can be seen in Figure 5. Figure 6 shows the dechirping strength of the corrugated plates as a function of plate separation. The blue line showing the dechirping strength was calculated by adding the wakefield-induced energy change (Equation 1 convolved with the bunch charge distribution and multiplied by the length of the dechirper) to the initial chirped beam. As the plate separation closes past a certain point, the theoretical dechirping strength peaks before reversing sign. This happens for two reasons. First, the beam gets over-dechirped and gains an increasing and oppositely-signed chirp. Second, the wavelength of the wakefield (Equation 1) shrinks to the extent that the wakefield is no longer linear. If the wakefield wavelength is sufficiently short, the bunch sees alternating positive and negative kicks along its length.

It can also be seen in Figure 6 that the measured dechirping power has the same behavior as the theoretical, but is weaker by about half. There are several possibilities for this that warrant further investigation:

- To what extent does the misalignment of the corrugations of the two plates reduce the strength of the dechirping wakefield? It was observed that the plates oscillated longitudinally by as much as half a corrugation period as they were actuated vertically (offset observable in Figure 4).

- Is the $\pi^2/16$ factor in Equations 1 and 3 sufficient to account for the different geometries (pipe vs. plates)?

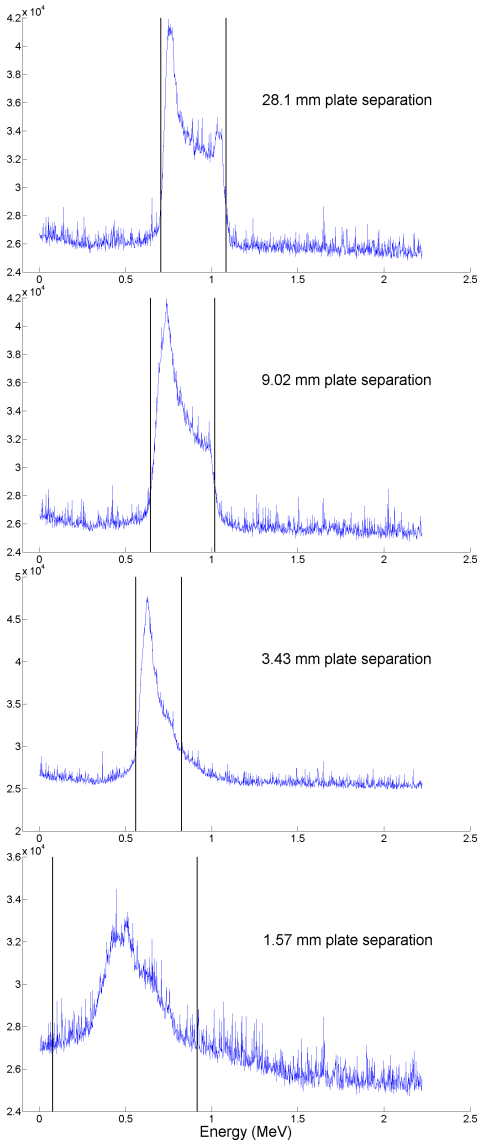

Figure 5: Energy spectrum plots at various plate separations. Note that closing the gap too much (smaller than ∼3.4 mm) results in a larger energy spread. The vertical lines designate the width where the intensity falls to 20% of the maximum height over the background.

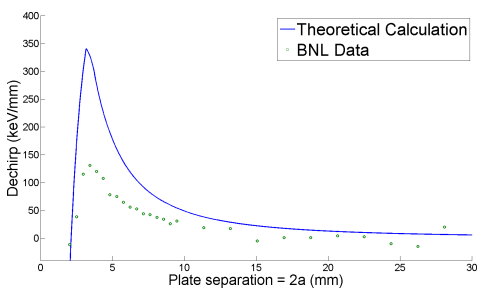

Figure 6: Dechirping Strength of parallel plates vs. Plate Separation, showing the measured dechirping strength at about half of theoretical predictions.

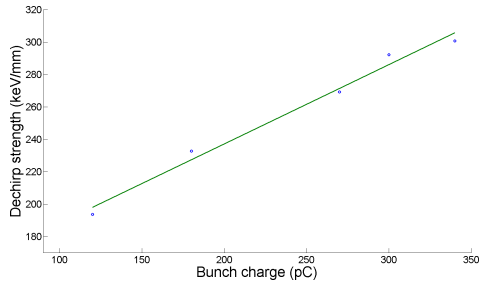

Figure 7: Dechirping Strength vs. bunch charge.

- How much of the measured energy spread is due to chirp, and how much is uncorrelated energy spread? The uncorrelated energy spread would result in an overestimation of the beam's initial chirp.

The result of the bunch charge variation experiment is shown in Figure 7. As expected, the relationship is linear.

FUTURE WORK

A second passive dechirping system is being planned that will involve a much longer corrugated plate section (>1 m) and an actuation system less prone to alignment errors. A longer dechirper is desirable because larger plate separations can be used, leading to longer wakefield wavelengths and a wider range of accepted bunch lengths. These are also more easily tuned by varying the plate separation for producing beams with near-zero chirp.

Furthermore, future experiments will make measurements with a deflecting cavity in addition to a dipole spectrometer to directly measure the beam's chirp. Transverse effects, especially any emittance blowup, will also be characterized.

ACKNOWLEDGMENTS

RadiaBeam Systems wishes to thank the staff at BNL ATF for their valuable assistance in this experiment. Special thanks to Karl Kusche and Christina Swinson for their personal involvement.

This is experiment is supported by an ongoing DOE Phase I Small Business Initiative for Research (SBIR) Grant, number DE–SC0009550.

REFERENCES

[1] K.L.F. Bane, G. Stupakov, Nucl. Inst. Meth. 690 (2012) 106–110.

[2] K. Bane, G. Stupakov, "Corrugated Pipe as a Beam Dechirper," SLAC-PUB-14925, April 2012.

[3] P. Emma, "Proposal for a Corrugated Beam Pipe Wakefield Experiment," NGLS Technical Note 24.

[4] K. Bane and A. Novokhatski, "The resonator impedance model of surface roughness applied to the LCLS parameters," LCLS-TN-99-1, SLAC, 1999.

[5] A. W. Chao, "Physics of collective beam instabilities in high energy accelerators" (John Wiley & Sons, New York, NY, 1993) 47–48.

ISBN 978-3-95450-138-0